

Contents lists available at ScienceDirect

# Sensors and Actuators: B. Chemical

journal homepage: www.elsevier.com/locate/snb





# Silicon ring resonator with ZIF-8/PDMS cladding for sensing dissolved CO<sub>2</sub> gas in perfluorocarbon solutions

Hyun-Tae Kim\*,1, Bibek Ramdam1, Miao Yu

Department of Mechanical Engineering, University of Maryland, College Park, MD 20742, USA

#### ARTICLEINFO

Keywords: Dissolved CO<sub>2</sub> sensor Silicon ring resonator ZIF-8 PDMS, perfluorocarbon

#### ABSTRACT

Precise measurement of dissolved  $CO_2$  gas concentration in perfluorocarbon (PFC) solution is essential to the implementation and understanding of extra-pulmonary gas exchange with liquid ventilation. While electrochemical and optochemical sensing methods are widely used for dissolved  $CO_2$  sensing in aqueous solution, dissolved  $CO_2$  sensing in the PFC solution remains largely unexplored. We report a refractive index-based silicon photonic sensor for monitoring dissolved  $CO_2$  gas in the PFC solution. The sensor employs a high-Q silicon ring resonator with ZIF-8 cladding for selective and sensitive detection of dissolved  $CO_2$  gas. Further, a gas-permeable PDMS coating layer is applied to the ZIF-8 cladding for enabling gas diffusion between the PFC solution and the ZIF-8. The PDMS layer does not dissolve in PFC and its hydrophobic properties help protect the ZIF-8 from potential damage caused by aqueous body fluids in the PFC solution during the liquid ventilation process. The fabricated sensor exhibits stable and repeatable responses in the PFC solution with a fine resolution of  $\sim 0.16 \ CO_2$  vol%, good selectivity for dissolved  $CO_2$  over dissolved  $CO_2$  and a fast response time of  $\sim 1.9$  min, enabling reliable monitoring of dissolved  $CO_2$  gas level changes in the PFC solution.

## 1. Introduction

Monitoring the concentration of dissolved CO<sub>2</sub> gas is important in various medical areas, particularly in extra-pulmonary gas exchange with liquid ventilation [1–3]. Extra-pulmonary gas exchange involves the use of alternative methods to facilitate gas exchange outside of the traditional lung-air interface. One such approach leverages the unique advantages of perfluorocarbons (PFCs) as facilitators for gas exchange [4]. PFCs exhibit valuable properties that render them well-suited for medical applications, including their inert nature due to the strength of the carbon-fluorine bond and their exceptional oxygen and carbon dioxide solubilities [5,6]. These properties make PFCs promising candidates for liquid ventilation [7–12]. To effectively implement and understand the liquid ventilation process, monitoring the dissolved CO<sub>2</sub> gas concentration in the PFC solution is essential [13].

Many efforts have been devoted to sensing dissolved  ${\rm CO_2}$  gas for a range of applications, including medical, environmental, and food process monitoring [14–18]. The most common approaches are based on electrochemical and optochemical sensors [19]. These sensors operate by allowing gas diffusion from the solution to the sensor head through a

gas-permeable membrane, which acts as a barrier between the sensor head and the solution. Electrochemical sensors employ an electrolyte with electrodes in the sensor head [20], while optochemical sensors utilize a polymer matrix incorporating fluorescence or luminescence materials that respond to CO2 molecules [21]. However, electrochemical sensors require regular and costly maintenance due to the aging of the electrolyte and they are relatively bulky for in-vivo monitoring. On the other hand, optochemical sensors based on an optical fiber offer a more compact and minimally invasive monitoring solution without the aging issue [14,22]. Nevertheless, both electrochemical and optochemical sensors are primarily designed to operate in aqueous solutions, limiting their use in PFC solutions. For example, the gas-permeable membrane used in these sensors is often made of Teflon, which dissolves in PFC solutions [22]. Additionally, the polymer matrix used in optochemical sensors may generate a signal drift when used in non-aqueous solutions [23].

Refractive index (RI)-based dissolved gas sensing is an alternative optical sensing approach. Unlike the optochemical sensing approach, which operates at a specific wavelength of light, RI-based sensing can be designed to work at any wavelength [24]. This versatility allows for the

 $<sup>\ ^{\</sup>ast}\ Corresponding\ authors.$ 

E-mail addresses: htkim@umd.edu (H.-T. Kim), mmyu@umd.edu (M. Yu).

<sup>&</sup>lt;sup>1</sup> These authors contributed equally.

utilization of low-cost optoelectronics designed for optical communication systems, such as light sources and detectors operating at the wavelength of 1.3  $\mu m$  and 1.55  $\mu m$  [25,26]. One of the drawbacks of RI-based sensing is the lack of selectivity to a target gas. This limitation can be successfully overcome by utilizing target gas-specific coating materials. For example, metal-organic-frameworks (MOFs), which selectively adsorb specific gas molecules based on their pore size [27], have shown promise in enabling selective and sensitive detection of target gases in RI-based sensing [28]. Specifically, ZIF-8 has been widely employed for selective detection of CO2 gas [29–31]. However, most of the ZIF-8-based sensors have primarily focused on CO2 sensing in gas environment due to the instability of ZIF-8 in aqueous solutions [32], and its application in dissolved CO2 sensing, particularly in PFC solution, remains unexplored.

In this paper, we present a RI-based silicon photonic sensor for measuring dissolved CO2 gas in PFC solution. The sensor employs a silicon ring resonator with a ZIF-8/PDMS top cladding layer, as shown in Fig. 1(a). Silicon photonics proves to be an excellent platform for developing ultracompact and cost-effective optical sensors due to the high refractive index contrast and compatibility with complementary metal-oxide-semiconductor (CMOS) fabrication processes [33,34]. The ring resonator allows for achieving high-Q resonance, enabling low detection limit RI sensing [35]. The resonance wavelength undergoes a shift corresponding to changes in the RI of the waveguide cladding layer. The ZIF-8 cladding layer enables selective and sensitive detection of the RI change induced by CO<sub>2</sub> adsorption in the ZIF-8 material [31]. Furthermore, the gas-permeable PDMS coating layer allows CO2 gas molecules to diffuse into and out of the ZIF-8 material while effectively separating the ZIF-8 from the PFC solution [Fig. 1(b)]. Note that PDMS does not dissolve in PFC solution [36]. Moreover, the hydrophobicity of PDMS helps protect the ZIF-8 from potential water-induced damage that might occur due to the aqueous body fluids mixed with the PFC solution during the liquid ventilation process. The effects of the PDMS coating layer on water-induced damage of the ZIF-8 are experimentally investigated, which will pave the way for research on MOFs for dissolved gas sensing in aqueous solutions. To the best of our knowledge, this work is the first attempt to measure dissolved CO2 gas in PFC solution using a ZIF-8-based RI sensor.

# 2. Materials and methods

## 2.1. Materials

A silicon-on-insulator (SOI) wafer with a 220 nm device layer and a 3  $\mu m$  buried oxide layer was employed for the silicon ring resonator fabrication. 950 PMMA A2 from MicroChem and ma-N 2403 from Micro Resist Technology were used as a resist material for e-beam lithography. Zinc nitrate hexahydrate (Zn(NO<sub>3</sub>)<sub>2</sub>·6 H<sub>2</sub>O) and 2-Methylimidazole (2-mIm) from Sigma-Aldrich were utilized for the ZIF-8 coating process. The PDMS coating was achieved using Sylgard  $^{\rm TM}$  184 Silicone Elastomer

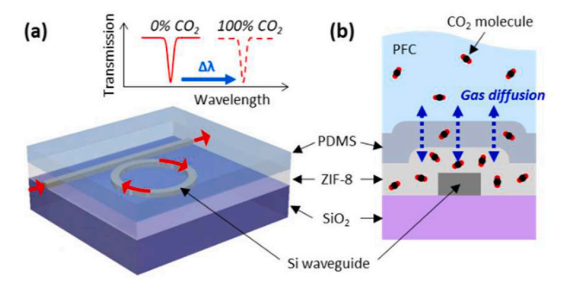


**Fig. 1.** Schematics showing (a) the dissolved  $CO_2$  sensor based on a silicon ring resonator and its signal shift in the transmission spectrum and (b) the diffusion of  $CO_2$  gas molecules across the ZIF-8/PDMS cladding layer.

Kit from Dow and hexane (HPLC Grade) from Fisher Chemical. Per-fluorodecalin ( $C_{10}F_{18}$ ) from FluoroMed L.P. was used for the PFC solution

#### 2.2. Silicon ring resonator fabrication

The SOI wafer was coated with a PMMA resist. Using e-beam lithography, the ring and bus waveguides and the grating couplers were patterned on the PMMA resist. A 20 nm Cr film was deposited on the patterned resist and then removed via a lift-off process with acetone. The Si device layer was then etched using reactive ion etching (RIE) with the Cr etch mask, followed by wet etching of the Cr mask. Four ring resonators were fabricated with radii of  $10~\mu m$ ,  $10.4~\mu m$ ,  $10.8~\mu m$ , and  $11.2~\mu m$  [Fig. 2(a) and (d)]. The waveguide had dimensions of  $500~m \times 220~m m$  and the coupling gap was 550~m m [Fig. 2(b)]. The grating coupler had a periodicity of 800~m m, a duty cycle of 50~% m, and an etch depth of 110~m m [Fig. 2(c)]. Next, a  $1~\mu m$  layer of  $5iO_2~m m$  was deposited on the wafer to serve as the top cladding [Fig. 2(d)]. Finally, as shown in Fig. 2(e), the circular area of the top oxide cladding on the ring resonator was removed using additional e-beam lithography with a ma-N resist and RIE with a Ni/Cr (25~m m/15~m m) etch mask.

## 2.3. ZIF-8/PDMS coating and sensor packaging

The SOI wafer with the fabricated ring resonators was coated with a ZIF-8 layer using the following procedure. Initially, the wafer was cleaned in a piranha solution for 30 min and then rinsed with deionized (DI) water and dried with N2 blow. A ZIF-8 coating solution was prepared by mixing methanolic solutions of Zn(NO<sub>3</sub>)<sub>2</sub>·6 H<sub>2</sub>O (1.25 mM) and 2-mIm (2.5 mM). The chip was immersed in the mixed solution for 30 min. Afterwards, the wafer was rinsed in methanol and dried with N2 blow. This coating procedure was repeated until the ZIF-8 thickness reached 1.5 µm. The thickness of the ZIF-8 layer was monitored using ellipsometry, with a dummy silicon wafer serving as a reference. The deposition rate was measured to be ~50.2 nm per coating cycle, and it took 30 cycles to reach the desired thickness of 1.5 µm [Fig. 3(a)]. Following the ZIF-8 coating, a thin film of PDMS was spin-coated on the wafer. To achieve a film thickness of less than 10 um, a PDMS solution was prepared by mixing PDMS base and curing agent at a ratio of 10:1. This PDMS solution was then further diluted with hexane at a ratio of 1:1. The spin-coating process was carried out at a speed of 3000 rpm to deposit a PDMS layer with a thickness of 7 µm. The coated PDMS layer was baked for 10 min at 125 °C for curing. Fig. 3(b) shows the PDMS thickness at different spinning speeds, measured using a profilometer on a dummy silicon wafer.

The ZIF-8/PDMS coated SOI wafer was integrated with input and output optical fibers, as shown in Fig. 3(c). For precise alignment, two 3D-printed fiber holders and a chip base were used to align the optical fibers at approximately 5° with respect to the grating coupler. The optical fibers were attached to the fiber holders, while the sensor was attached to the chip base using a UV curable glue (OrmoComp, Micro Resist Technology). Once the alignment was achieved, the UV glue was applied between the fiber end face and the grating coupler, and UV light was applied to cure the glue. Finally, the 3D-printed fiber holders were bonded to the chip base using the UV glue.

## 2.4. Experimental setup

The fabricated sensor was characterized using the experimental setup shown in Fig. 4. To obtain the sensor signal, a tunable laser source (TSL-510, Santec), a polarization controller (FPC030, Thorlabs), and a photoreceiver (2053-FC, New Focus) were used. The output voltage from the photoreceiver was monitored with a data acquisition instrument (SPU-100, Santec for transmission spectrum measurement and PicoScope 6000, Pico Technology for dynamic response measurement). Dissolved gas sensing was carried out with CO<sub>2</sub> and O<sub>2</sub> as a test gas and

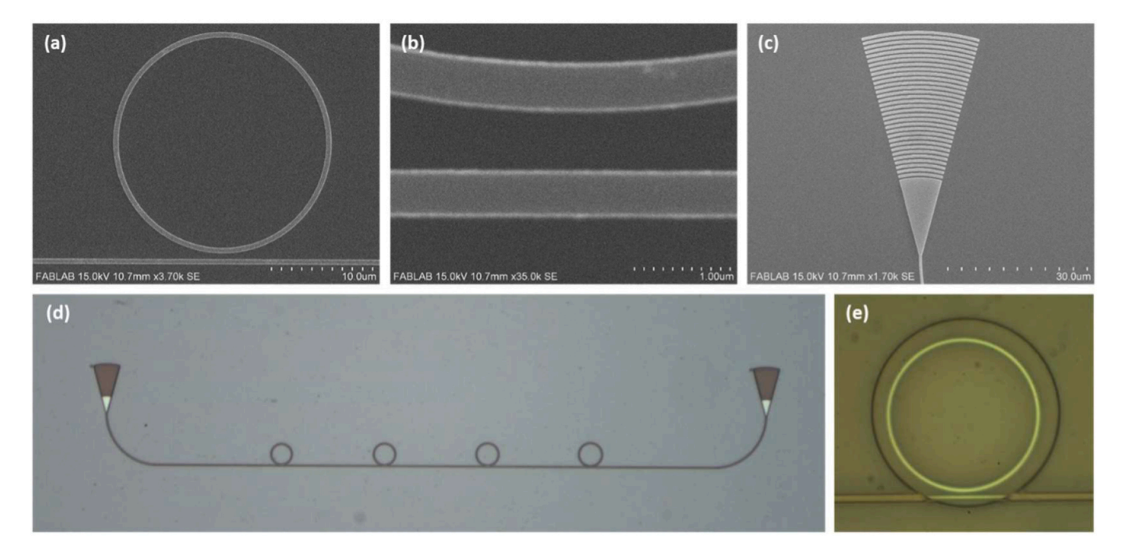


Fig. 2. SEM images of (a) the fabricated silicon ring resonator, (b) coupling region of the ring resonator, and (c) grating coupler. The images were taken before the deposition of the top oxide cladding layer. Optical microscope images of (d) cascaded four ring resonators and grating couplers with a top oxide cladding layer and (e) a representative ring resonator with a circular opening in the top oxide cladding.

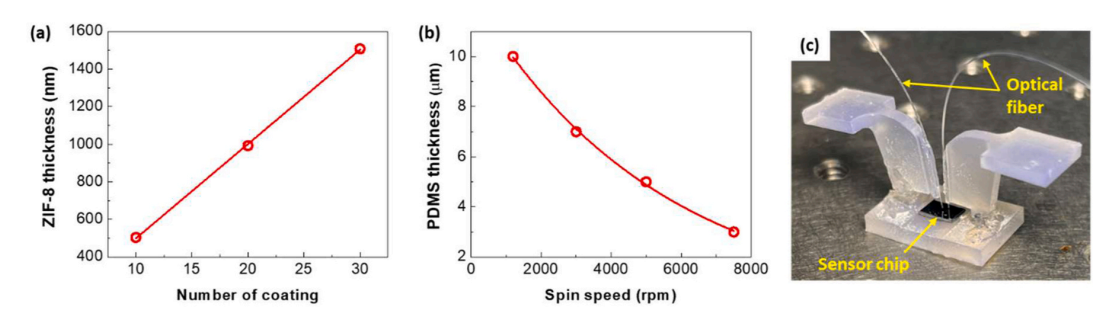


Fig. 3. (a) Measured thicknesses of the ZIF-8 film on a Si substrate with different numbers of coating cycle. (b) Measured thicknesses of the spin-coated PDMS film on a Si substrate with different spin speeds. (c) Dissolved CO<sub>2</sub> sensor chip packaged with aligned optical fibers.

 $N_2$  as a carrier gas. The flow rates of  $CO_2$ ,  $O_2$ , and  $N_2$  gases were controlled using mass flow controllers (6A0107SV-CA, 6A0107BV-OB, 6A0107BV-NC, Dakota Instruments). A solenoid valve (2W025–08, ATO Inc.) was installed between the test gas cylinder and the MFC for precise timing control of the gas flow. The valve was used only for characterizing the dynamic response of the sensor in gas environment.

Two sensor chambers were prepared to characterize the sensor response in the gas environment and the PFC solution. For the gas environment, the sensor was placed inside a hollow glass tube through which a controlled gas flow was passed, as shown in Fig. 4(b). For testing in the PFC solution, the sensor was placed on a glass beaker containing the PFC solution and the controlled gas was bubbled into the PFC solution, as shown in Fig. 4(c). Note that the gas tube outlet was positioned at a sufficient distance from the sensor to ensure that the gas bubbles do not directly contact with the sensor.

## 3. Results and discussions

## 3.1. Effects of the PDMS coating on the water-induced damage of ZIF-8

To investigate the protective properties of the PDMS coating on the water-induced damage of ZIF-8, silicon substrates with a 1  $\mu$ m thick ZIF-8 coating layer were prepared. These substrates were further coated with three different thicknesses of PDMS layer: 5  $\mu$ m, 7  $\mu$ m, and 10  $\mu$ m. Additionally, a reference sample with a 1  $\mu$ m thick ZIF-8 layer without

any PDMS coating was prepared for comparison. The prepared samples were then immersed in DI water.

As shown in Fig. 5, the water-induced damage of ZIF-8 became evident in the reference sample, where cracks started to appear on the ZIF-8 film after 1 h of immersion. As time progressed, the cracks increased and after 80 h in DI water, the ZIF-8 film was eliminated from the silicon substrate. In contrast, the samples with a PDMS coating layer showed a delay in the water-induced damage. For the 5 µm thick PDMS sample, cracks were observed after 1 h, but the density of cracks was significantly lower compared to the reference sample. As time passed, the cracks increased, and white spots appeared in the sample. The white spots could be attributed to empty spaces beneath the PDMS layer resulting from the ZIF-8 cracking or damage. After 4 h of immersion, the number and size of the white spots increased. Similar trends were observed for the samples with a thicker PDMS layer. In the case of the 7 μm thick PDMS sample, white spots began to appear after 10 h of immersion, while no spots were observed even after 10 h in the 10 µm thick PDMS sample. However, with prolonged immersion (after 80 h), small black dots appeared, which are believed to be indicative of ZIF-8 damage.

Overall, the PDMS coating layer showed a beneficial effect in delaying the water-induced damage of ZIF-8, with the thicker PDMS layers providing increased protection. However, even with the protective effect of PDMS, prolonged immersion led to the appearance of ZIF-8 damage in the form of black dots. Using a thicker PDMS coating layer

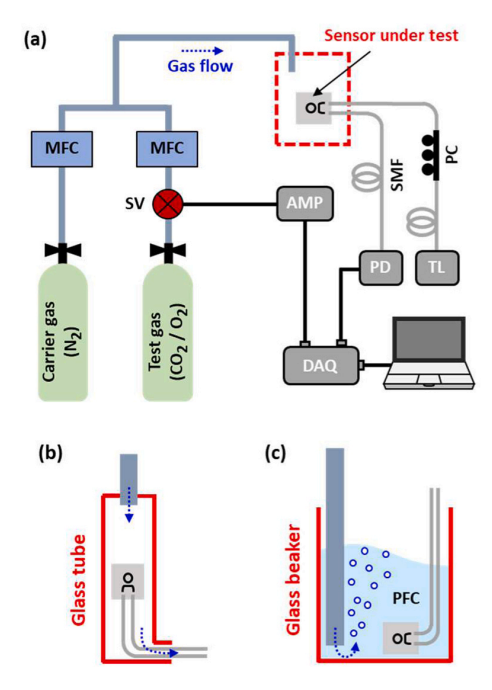


**Fig. 4.** (a) Experimental setup for the sensor characterization. AMP: amplifier, DAQ: data acquisition instrument, MFC: mass flow controller, PC: polarization controller, PD: photoreceiver, SMF: single-mode optical fiber, SV: solenoid valve, TL: tunable laser source. Schematic of the setup for testing the sensor in (b) the gas environment and (c) the PFC solution.

could further increase the protection time. However, it may result in a slower sensor response time due to the longer gas diffusion time through a thicker PDMS layer. Note that the PDMS coating layer does not influence the measured gas concentration due to its gas-permeability and the steady-state response of the sensor remains unaffected. In the current work, a 7  $\mu m$  thick PDMS coating layer was chosen for the sensor fabrication. Since the sensor was intended to operate primarily in the PFC solution, which could contain low levels of aqueous body fluids from the liquid ventilation process, the 7  $\mu m$  thick PDMS coating was expected to provide extended protection for the ZIF-8 film beyond the observed 10 h.

# 3.2. Sensor transmission spectrum and RI sensitivity

Fig. 6(a) and (b) show the transmission spectra of the fabricated sensor measured in air. It has a series of resonance dips from the four ring resonators. At approximately 1574 nm, the transmission spectrum exhibits the maximum output voltage with four distinctive resonance dips, each spaced ~1 nm apart. The free-spectral-ranges (FSRs) of the resonators with radii of 10 μm, 10.4 μm, 10.8 μm, and 11.2 μm were measured to be approximately 11.0 nm, 10.6 nm, 10.3 nm, and 9.8 nm, respectively. Although the grating coupler has a maximum coupling efficiency around 1560 nm, the stronger output signals observed around 1574 nm were primarily influenced by the spectral profile of the tunable laser source. Due to the stronger output voltage and the absence of overlap, the dips around 1574 nm were chosen for sensing purposes. It can be observed that the sensor spectrum measured in air changed after immersion in the PFC solution. The resonance dips shifted and the extinction at the resonances became deeper [Fig. 6(b)]. These changes in the sensor spectrum were observed only during the initial use of the sensor in the PFC solution. Subsequently, the sensor spectrum remained stable over multiple uses in the PFC solution. It is believed that the initial interaction between the PDMS and the PFC solution led to swelling of the PDMS, which in turn affected the cladding characteristics of the ring

resonators. Particularly, a resonance dip at  $\sim$ 1574 nm exhibits a deep extinction of  $\sim$ 20 dB with a high Q factor of 11,000. This dip was selected for dissolved CO<sub>2</sub> sensing.

Before the coating of ZIF-8/PDMS on the ring resonator, the RI sensitivity of the resonator was measured by covering it with different RI solutions [Inset of Fig. 6(c)]. Salt solutions with different salinities were used for the different RI solutions. The resonance shift at each RI was measured, as shown in Fig. 6(c), and the RI sensitivity was determined to be 146.9 nm/RIU. However, the presence of a thin residual oxide layer on the silicon waveguide significantly reduced the RI sensitivity [Fig. 6 (d) and (e)]. This thin oxide layer was intentionally left to prevent damage to the waveguide during the RIE process of the top oxide layer. The simulation results [Fig. 6(e)] indicate that the measured RI sensitivity of ~146.9 nm/RIU is resulted from a residual oxide thickness of approximately 60 nm. A RI sensitivity of 229.8 nm/RIU is obtainable by completely removing the residual oxide layer. A gas-phase hydrofluoric acid etch process can be a potential solution to address this issue. This process enables selective and complete removal of the top oxide layer without damaging the silicon waveguide.

#### 3.3. Sensor response in the gas environment

The fabricated sensor was characterized first in the gas environment and the sensitivity, resolution, and response time of the sensor were obtained. The sensor was placed inside the glass tube and stabilized under a continuous flow of  $N_2$  gas for 12 h prior to testing. The  $N_2$  blow process was intended to eliminate methanol residuals, which are a byproduct of the fabrication process, from the ZIF-8 layer. This process can be replaced with a single dynamic vacuum drying session at 120 °C for 12 h, immediately following the ZIF-8 coating [37]. Following the stabilization period, different concentrations of test gas were introduced into the glass tube. Fig. 7(a) shows the resonance shift of the sensor at different gas concentrations. The sensor exhibits a CO<sub>2</sub> sensitivity of  $\sim$ 8.7 pm/CO<sub>2</sub> vol% and negligible responses to O<sub>2</sub> gas.

To evaluate the sensing resolution, the resonance wavelength was monitored in room temperature air over 1 h with a measurement interval of 1 min, as shown in Fig. 7(b). The standard deviation of the resonance shift was measured to be 1.4 pm, which is the wavelength resolution of the sensor. Based on this wavelength resolution, the  $CO_2$  sensing resolution was calculated to be  $\sim 0.16$   $CO_2$  vol%.

For the response time measurement, the tunable laser wavelength was fixed at ~1574 nm, which corresponds to the steep slope of the resonance. The sensor was subjected to a continuous flow of N<sub>2</sub> at a rate of 5 l/min. To induce a fast and small change in the CO<sub>2</sub> concentration, a step voltage input was introduced to the solenoid valve to obtain a CO2 flow rate of 1 l/min [Fig. 7(c)]. The PD output voltage was recorded with a sampling rate of 1 msec. The 10-90 % response and recovery times were measured to be ~2.6 msec and ~2.4 msec, respectively. Note that the measured response time includes both the response of the sensor itself and the response of the gas handling system, which includes factors such as flow rate-dependent manifold mixing and solenoid valve actuation. Therefore, the actual response and recovery times of the sensor are expected to be smaller than the measured values. In our future work, an optimization-based system identification method is planned to precisely characterize the dynamics of the gas handling system based on the measured responses.

## 3.4. Sensor response in the PFC solution

The sensor was initially placed in an empty glass beaker. Subsequently, 45 ml of PFC solution was poured into the beaker, submerging the sensor in the PFC solution. The resonance wavelength of the sensor was monitored every 1 min throughout the PFC response testing.

Fig. 8(a) shows the time response of the resonance wavelength shift of the sensor. When  $N_2$  gas was blown into the PFC solution, the resonance wavelength showed a blueshift. Following the  $N_2$  gas blow, the  $N_2$ 

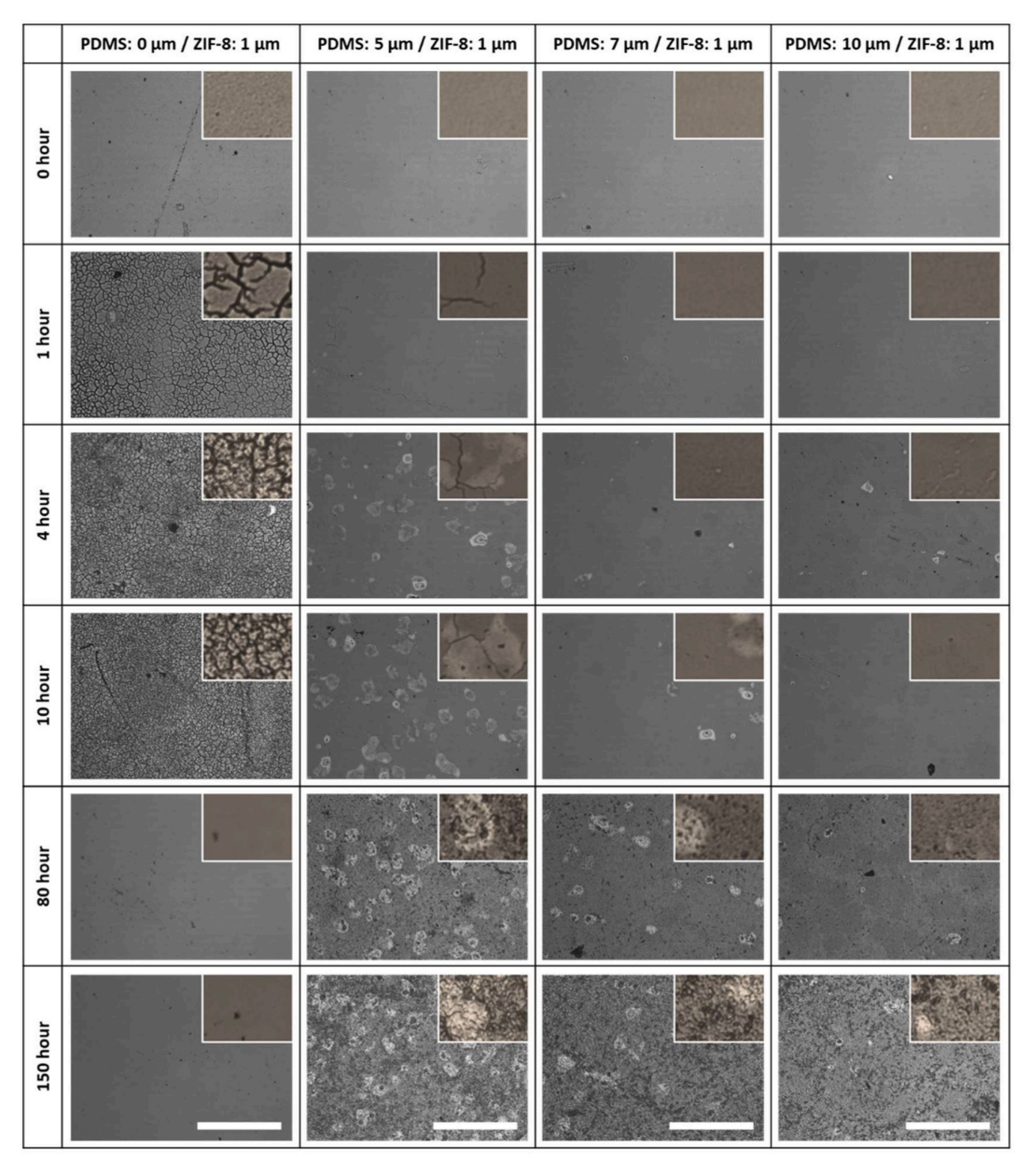


Fig. 5. Optical microscope images of ZIF-8 (thickness:  $1 \mu m$ ) coated silicon substrates with different thicknesses of PDMS coating. The images with 20 times magnification were taken before (0 h) and after being immersed in DI water for 1 h, 4 h, 10 h, 80 h, and 150 h. The white scale bars represent 100  $\mu m$ . The insets in the top-right corner of each image are 10 times zoom-in of the original image.

supply was cut off, and test gases, i.e.,  $CO_2$  and  $O_2$ , were introduced into the PFC solution. In this scenario, the resonance wavelength exhibited a redshift of approximately 0.88 nm in response to the  $CO_2$  blow, while the sensor did not respond to the  $O_2$  blow. The observed resonance shift of  $\sim$ 0.88 nm for the  $CO_2$  blow and no shift for the  $O_2$  blow are consistent with the resonance shifts observed in the gas environment. Furthermore, the cyclic test results demonstrate that the sensor has good repeatability in its response to dissolved  $CO_2$  gas. As our sensor is designed to operate in PFC solutions containing only  $CO_2$  and  $O_2$  gases during the liquid ventilation process, the demonstrated selectivity is sufficient for this application. However, given that ZIF-8 also responds to volatile organic compounds (VOCs) [37], in other applications with the presence of VOCs, the crosstalk from VOCs may affect the  $CO_2$  selectivity of the sensor. This crosstalk issue can be addressed by employing an array of

ring resonators, each functionalized with a different type of MOF that has a distinctive response to  $\text{CO}_2$  and VOCs.

The 10–90 % response and recovery times of the sensor in the PFC solution were measured to be  $\sim\!5.1$  min and  $\sim\!4.2$  min, respectively at a flow rate of 1 l/min. The response time was found to decrease with increasing CO<sub>2</sub> flow rate, as shown in Fig. 8(b). At a flow rate of 2 l/min, the response time reduced to  $\sim\!3.3$  min. These response times are limited by both the time for CO<sub>2</sub> bubbles to be dissolved in the PFC solution and the time for dissolved CO<sub>2</sub> gas to diffuse into the ZIF-8 layer, which are much slower than the millisecond level of sensor response time in the gas environment [Fig. 7(c)]. As the response time of sensor itself is in milliseconds, the fabricated sensor is believed to be fast enough to reliably monitor changes in the dissolved CO<sub>2</sub> gas level in the PFC solution for the liquid ventilation process. It should be noted that the

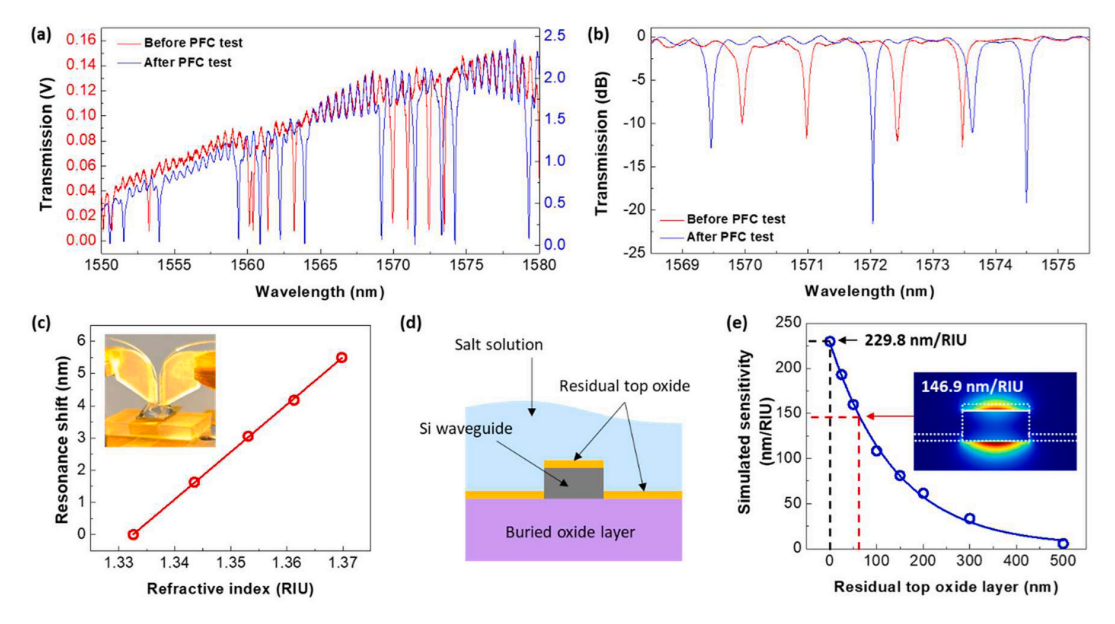


Fig. 6. (a) Transmission spectra of the sensor before and after testing in the PFC solution and (b) the zoom-in view of the four resonance dips around 1574 nm wavelength. Both spectra were measured in air. (c) Measured resonance shift of the ring resonator with respect to different RIs of salt solution. The inset shows the ring resonator under testing with the salt solution on top. (d) Schematic of the cross-sectional view of the silicon waveguide with a residual top oxide layer. (e) Simulated RI sensitivity of the ring resonator with respect to different thicknesses of residual top oxide layer. The inset shows the mode profile of the silicon waveguide with a 60 nm thick top oxide layer.

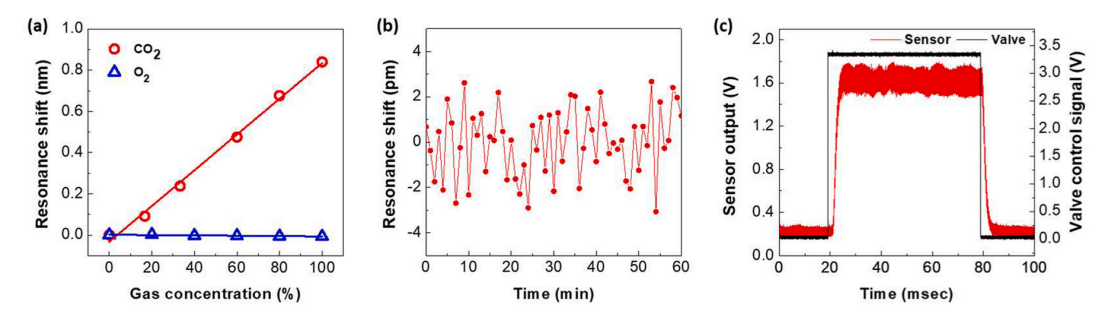


Fig. 7. (a) Resonance shift of the sensor measured in  $CO_2$  and  $O_2$  gases with different gas concentrations. (b) Measured sensor noise in room temperature air. (c) Dynamic response of the sensor when the  $CO_2$  gas concentration in the glass tube changes from 0 % to 16.7 % and then back to 0 %.

sensor performance showed no degradation over the course of the 16.7-hour sensor response experiment in the PFC solution [Fig. 8(a) and (b)]. These results demonstrate the excellent stability of the ZIF-8/PDMS coating layer in the PFC solution.

Additionally, the dynamic response of the sensor was characterized in PFC solutions with different CO2 concentrations. For the experiment, two PFC solutions were prepared: one was blown with N2 gas and the other with  $CO_2$  gas for 20 min at a flow rate of 1 l/min. These  $N_2$ - and CO<sub>2</sub>-saturated PFC solutions were then mixed in different volume ratios to achieve 0 %, 10 %, 20 %, 50 %, and 100 % CO2 concentrations in the PFC solutions. For example, a PFC solution with a 50 % CO2 concentration was obtained by mixing equal volumes of N2- and CO2-saturated PFC solutions. The mixed PFC solution was immediately transferred into the beaker containing the sensor. Fig. 8(c) shows the dynamic response of the sensor to PFC solutions with different CO2 concentrations. For a concentration of 100 %, the resonance wavelength swiftly redshifted, reaching a maximum shift of ~0.78 nm within 2 min of the sensor immersion in the PFC solution. Subsequently, the resonance wavelength exhibited a blueshift, which is believed to be due to the degasification of dissolved CO<sub>2</sub> from the PFC solution. The 10–90 % response time was measured to be ~1.9 min, which was slower than a response time of

~2.6 msec in the gas environment. The faster response time in the gas environment is attributed to CO2 having a higher diffusivity in air than in a liquid, such as a PFC solution [38]. A similar trend was observed for lower CO2 concentrations. The maximum resonance shift (at time t = 21 min) was found to decrease linearly with a decrease in CO2 concentration, as shown in Fig. 8(d). The sensitivity was obtained to be ~7.8 pm/CO<sub>2</sub> vol%, which was lower than the ~8.7 pm/CO<sub>2</sub> vol% measured in the gas environment [Fig. 7(a)]. As these results [Fig. 8(c) and (d)] were obtained 8 months after those of Figs. 7(a) and 8(a), the steady-state responses to the CO2-saturated PFC solution obtained at different times were compared, as shown in Fig. 8(e). The steady-state resonance shift obtained after 8 months was found to be ~0.1 nm smaller. This indicates that the lower sensitivity was a result of sensor performance degradation, which may be due to damage to the ZIF-8 caused by ambient moisture diffusing into the ZIF-8 via the PDMS layer. Note that the use of the same sensor for multiple tests to evaluate its response in the PFC solution demonstrated that the sensor is both reusable and capable of producing reproducible results. However, since the sensor is intended for medical applications, it will not be reused to prevent any potential harm that could arise from biocontamination.

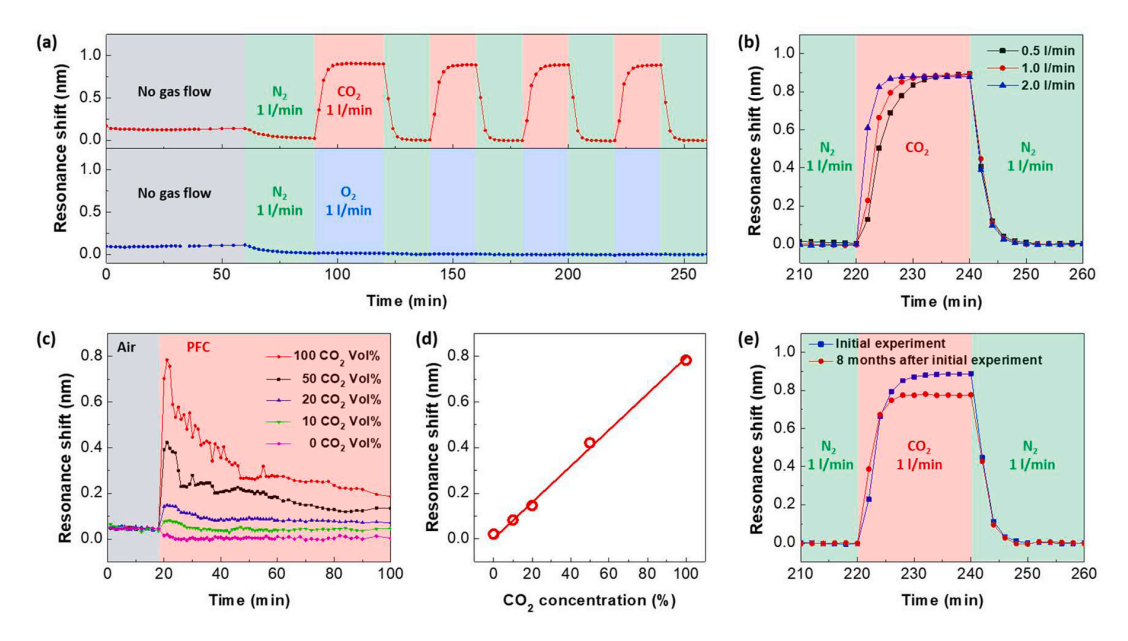


Fig. 8. (a) Dynamic response of the sensor in the PFC solution before and after gas blow into the PFC solution (gray zone: no gas flow, green zone: N2 gas with a 1 l/ min of flow rate, red zone: CO<sub>2</sub> gas with a 1 l/min of flow rate, blue zone: O<sub>2</sub> gas with a 1 l/min of flow rate). (b) Dynamic response of the sensor in PFC solutions with different flow rates of CO2 gas. (c) Dynamic response of the sensor in PFC solutions with different CO2 concentrations and (d) maximum resonance shift (obtained at t = 21 min) with respect to CO<sub>2</sub> concentration. (e) Comparison of the dynamic responses of the sensor over an 8-month period. (a) and (b) were obtained from the initial experiments. (c) and (d) were obtained with the same sensor 8 months after the initial experiments.

#### 4. Conclusions

We successfully developed a silicon photonic sensor with a ZIF-8/ PDMS cladding layer for dissolved CO2 gas sensing in PFC solutions. The sensor was demonstrated to have a fine resolution of ~0.16 CO₂ vol % for measuring CO2 gas and good selectivity that allows effective distinguishment from dissolved O2 gas. The sensor was also shown to have response and recovery times of ~2.6 msec and ~2.4 msec in the gas environment and a response time of ~1.9 min in the PFC solution. Based on our previous animal experiment for liquid ventilation [13], the CO2 level change in PFC solution is expected to be ~5.5 CO2 vol% and this  $CO_2$  level change is expected to occur slowly over  $\sim$  6.7 min. Therefore, our sensor will allow for reliable monitoring of the dissolved CO2 level change for the liquid ventilation processes. For performance comparison, one of the commercially available optochemical sensors for dissolved CO2 measurement has a measurement range of 1-25 CO2 vol%, a resolution of ~0.15 CO2 vol% at 6 CO2 vol%, and a response time of  $\sim$ 3 min [23]. Moreover, the PDMS coating layer was proved to serve as protection for the ZIF-8 from potential water-induced damage. It should be noted that while the current sensor specifically measures dissolved CO<sub>2</sub> gas using ZIF-8, the proposed sensing approach would enable simultaneous measurement of multiple dissolved gases by employing an array of ring resonators, each coated with different MOFs that respond distinctively to target gases. In addition, the sensor size can be further miniaturized by integrating the sensor chip onto the end-face of an optical fiber as in [39]. This will lead to the development of an ultracompact fiber-optic sensor for simultaneous measurements of multiple dissolved gases, which would benefit various applications, including medical, environmental, and food process monitoring.

## CRediT authorship contribution statement

Hvun-Tae Kim: Conceptualization, Formal analysis, Investigation, Methodology, Software, Supervision, Validation, Visualization, Writing - original draft. Bibek Ramdam: Data curation, Formal analysis, Investigation, Methodology, Software, Validation, Visualization,

Writing - original draft. Miao Yu: Conceptualization, Funding acquisition, Project administration, Resources, Supervision, Writing - review & editing.

# **Declaration of Competing Interest**

The authors declare that they have no known competing financial interests or personal relationships that could have appeared to influence the work reported in this paper.

## Data availability

Data will be made available on request.

# Acknowledgments

This work was partially supported by the National Science Foundation (USA) Growing Convergence Research (GCR) program (OIA2121110) and National Institute of Food and Agriculture (USA) Sustainable Agricultural Systems (SAS) program (20206801231805).

## References

- [1] S.R. Carr, J.P. Cantor, A.S. Rao, T.V. Lakshman, J.E. Collins, J.S. Friedberg, Peritoneal perfusion with oxygenated perfluorocarbon augments systemic oxygenation, Chest 130 (2006) 402-411.
- [2] J.L. Leibowitz, W. Naselsky, M. Doosthosseini, K. Aroom, A. Shah, G.J. Bittle, et al., Extrapulmonary gas exchange through peritoneal perfluorocarbon perfusion J. Clin. Transl. Sci. 6 (2022) 34.
- [3] J.L. Leibowitz, M.A. Awad, S. Stachnik, Y. Moon, B. Kadkhodaeielyaderani, J. O. Hahn, et al., Oxygenated peritoneal perfluorodecalin improves response to normobaric hypoxic exposure in swine, J. Clin. Transl. Sci. 7 (2023) 96.
  [4] T.C. Fabian, Perfluorocarbons, J. Trauma Acute Care Surg. 70 (2011) \$42–\$44.
- K.C. Lowe, Properties and Biomedical Applications of Perfluorochemicals and Their Emulsions, Organofluorine Chemistry: Principles and Commercial Applications Springer, 1994, pp. 555-577.
- [6] J.G. Riess, Understanding the fundamentals of perfluorocarbons and perfluorocarbon emulsions relevant to in vivo oxygen delivery, Artif. Cells, Blood Substit., Biotechnol. 33 (2005) 47-63.

- [7] I.P. Torres Filho, Mini-review: perfluorocarbons, oxygen transport, and microcirculation in low flow states: in vivo and in vitro studies, Shock 52 (2019) 19-27
- [8] B.D. Spiess, Perfluorocarbon gas transport: an overview of medical history with yet unrealized potentials. Shock 52 (2019) 7–12.
- [9] C. Bialas, C. Moser, C.A. Sims, Artificial oxygen carriers and red blood cell substitutes: a historic overview and recent developments toward military and clinical relevance, J. Trauma Acute Care Surg. 87 (2019) S48–S58.
- [10] J.S. Jahr, N.R. Guinn, D.R. Lowery, L. Shore-Lesserson, A. Shander, Blood substitutes and oxygen therapeutics: a review, Anesth. Analg. 132 (2020) 119–129.
- [11] R. Leonard, Liquid ventilation, Anaesth. Intensive Care 26 (1998) 11–21.
- [12] U. Kaisers, K.P. Kelly, T. Busch, Liquid ventilation, Br. J. Anaesth. 91 (2003) 143–151.
- [13] M. Doosthosseini, K.R. Aroom, M.R. Aroom, M. Culligan, W. Naselsky, C. Thamire, et al., Monitoring, control system development, and experimental validation for a novel extrapulmonary respiratory support setup, IEEE/ASME Trans. Mechatron. 27 (2022) 4177–4187.
- [14] J.J. Davenport, M. Hickey, J.P. Phillips, P.A. Kyriacou, A fiberoptic sensor for tissue carbon dioxide monitoring, in: Proceedings of the 2015 37th Annual International Conference of the IEEE Engineering in Medicine and Biology Society (EMBC), IEEE 2015, pp. 7942–7945.
- [15] J.S. Clarke, E.P. Achterberg, D.P. Connelly, U. Schuster, M. Mowlem, Developments in marine pCO2 measurement technology; towards sustained in situ observations, TrAC Trends Anal. Chem. 88 (2017) 53–61.
- [16] X. Meng, S. Kim, P. Puligundla, S. Ko, Carbon dioxide and oxygen gas sensors-possible application for monitoring quality, freshness, and safety of agricultural and food products with emphasis on importance of analytical signals and their transformation, J. Korean Soc. Appl. Biol. Chem. 57 (2014) 723–733.
- [17] T. Lang, T. Hirsch, C. Fenzl, F. Brandl, O.S. Wolfbeis, Surface plasmon resonance sensor for dissolved and gaseous carbon dioxide, Anal. Chem. 84 (2012) 9085–9088.
- [18] Y. Ma, L.-Y.L. Yung, Detection of dissolved  $CO_2$  based on the aggregation of gold nanoparticles, Anal. Chem. 86 (2014) 2429–2435.
- [19] J. Zosel, W. Oelßner, M. Decker, G. Gerlach, U. Guth, The measurement of dissolved and gaseous carbon dioxide concentration, Meas. Sci. Technol. 22 (2011) 273021
- [20] S. Yao, M. Wang, Electrochemical sensor for dissolved carbon dioxide measurement, J. Electrochem. Soc. 149 (2001) H28.
- [21] S.M. Borisov, R. Seifner, I. Klimant, A novel planar optical sensor for simultaneous monitoring of oxygen, carbon dioxide, pH and temperature, Anal. Bioanal. Chem. 400 (2011) 2463–2474.
- [22] G. Neurauter, I. Klimant, O.S. Wolfbeis, Fiber-optic microsensor for high resolution pCO 2 sensing in marine environment, Fresenius' J. Anal. Chem. 366 (2000) 481–487.
- [23] Pre Sens, PreSens carbon dioxide sensor. (https://www.presens.de/products/det ail/co2-sensor-spot-sp-cd1).
- [24] A. Shadab, S.K. Raghuwanshi, S. Kumar, Advances in micro-fabricated fiber Bragg grating for detection of physical, chemical and biological parameters—a review, IEEE Sens. J. (2022).
- [25] G. Masini, L. Colace, G. Assanto, Si based optoelectronics for communications, Mater. Sci. Eng.: B 89 (2002) 2–9.

- [26] S. Fama, L. Colace, G. Masini, G. Assanto, H.-C. Luan, High performance germanium-on-silicon detectors for optical communications, Appl. Phys. Lett. 81 (2002) 586–588.
- [27] B. Chen, S. Xiang, G. Qian, Metal—organic frameworks with functional pores for recognition of small molecules, Acc. Chem. Res. 43 (2010) 1115–1124.
- [28] C. Zhu, R.E. Gerald, J. Huang, Metal-organic framework materials coupled to optical fibers for chemical sensing: a review, IEEE Sens. J. 21 (2021) 19647–19661.
- [29] K.-J. Kim, P. Lu, J.T. Culp, P.R. Ohodnicki, Metal-organic framework thin film coated optical fiber sensors: a novel waveguide-based chemical sensing platform, ACS Sens. 3 (2018) 386–394.
- [30] H.-T. Kim, W. Hwang, Y. Liu, M. Yu, Ultracompact gas sensor with metal-organic-framework-based differential fiber-optic Fabry-Perot nanocavities, Opt. Express 28 (2020) 29937–29947.
- [31] B. Chocarro-Ruiz, J. Pérez-Carvajal, C. Avci, O. Calvo-Lozano, M.I. Alonso, D. Maspoch, et al., A CO 2 optical sensor based on self-assembled metal-organic framework nanoparticles, J. Mater. Chem. A 6 (2018) 13171–13177.
- [32] H. Zhang, M. Zhao, Y. Lin, Stability of ZIF-8 in water under ambient conditions, Microporous Mesoporous Mater. 279 (2019) 201–210.
- [33] Q. Xu, D. Fattal, R.G. Beausoleil, Silicon microring resonators with 1.5-μm radius, Opt. Express 16 (2008) 4309–4315.
- [34] W. Bogaerts, R. Baets, P. Dumon, V. Wiaux, S. Beckx, D. Taillaert, et al., Nanophotonic waveguides in silicon-on-insulator fabricated with CMOS technology, J. Light. Technol. 23 (2005) 401.
- [35] M.S. Luchansky, R.C. Bailey, High-Q optical sensors for chemical and biological analysis, Anal. Chem. 84 (2012) 793–821.
- [36] J.N. Lee, C. Park, G.M. Whitesides, Solvent compatibility of poly (dimethylsiloxane)-based microfluidic devices, Anal. Chem. 75 (2003) 6544–6554.
- [37] J. Tao, X. Wang, T. Sun, H. Cai, Y. Wang, T. Lin, et al., Hybrid photonic cavity with metal-organic framework coatings for the ultra-sensitive detection of volatile organic compounds with high immunity to humidity, Sci. Rep. 7 (2017) 41640.
- [38] W.M. Haynes, CRC Handbook of Chemistry and Physics, CRC Press, 2014.
- [39] C.L. Arce, K. De Vos, T. Claes, K. Komorowska, D. Van Thourhout, P. Bienstman, Silicon-on-insulator microring resonator sensor integrated on an optical fiber facet, IEEE Photonics Technol. Lett. 23 (2011) 890–892.

**Hyun-Tae Kim** received the Ph.D. degree in mechanical engineering from the University of Maryland, College Park, MD, USA, in 2017. He is currently an Assistant Research Professor with the Department of Mechanical Engineering, University of Maryland, College Park. His research interests include optical sensors, micro/nano fabrication, and MEMS/NEMS.

**Bibek Ramdam** received his B.Sc. (2019) and M.S. (2022) in Mechanical Engineering both from Howard University. He is currently a Ph.D. student at the University of Maryland, College Park. His research focuses on nanophotonic sensors for gas sensing applications.

Miao Yu received her Ph.D. in Mechanical Engineering from the University of Maryland in 2002. She is currently a professor in the Department of Mechanical Engineering at the University of Maryland. Her research interests include sensors and actuators, photonics, wave-matter interaction, and acoustics. She is a fellow of ASME.